Journal of NAMP 72, (2026) 135-146

The Nigerian Association of Mathematical Physics

Journal homepage: https://nampjournals.org.ng

SYSTEM TRANSFER FUNCTION OF A PARABOLIC SOLAR DISH CONCENTRATOR USING FOURIER TRANSFORM.

[1]Osaisai, D. T, and [2]Azi, S. O

[1]Departmentof Physics, Faculty of Science, Niger Delta University, Amassoma, Bayelsa State
[2]Department of Physics, University of Benin, Benin City

ARTICLE INFO

Article history:
Received xxxxx
Revised xxxxx
Accepted xxxxx
Available online xxxxx

Keywords:
Solar Radiation, Parabolic solar dish, concentrator, Transfer Function, Fourier transform.

ABSTRACT

The sun produces vast amount of renewable solar energy, an inexhaustible resource that can be converted into heat and electricity. In this work, solar dish concentrator with diameter 2.35m for water heating application was designed using the parabolic solar concentrators for low and medium temperature application in different parts of the world. The interior surface of the dish was covered with reflecting mirrors of reflectivity up to 94 % and equipped with a receiver (boiler) located at the focal point. The water temperature increased to 90°C and a high receiver temperature of 160°C was recorded. Fourier transform was also carried out in MATLAB to obtain a transfer function for the measurement on Day 1. This model is used to predict subsequent water temperatures and receiver temperatures for Day 2 to Day 5. Results showed that the predicted water and receiver temperatures followed the same trend as the original values. Solar power/intensity and temperatures measurement were manually tracked. The limited accuracy resulted from hourly averages in operating conditions during the test and data acquisition.

1. INTRODUCTION

Energy is an essential ingredient of socio-economic development and economic growth [1]. The development of efficient and reliable Concentrating Solar Power (CSP) technologies has led to an increasing ability to focus and harness solar energy. The available solar energy from a system may depend on many factors such as the load, the collection and sizes, the operation, and the climate. Heat production from solar energy can be accomplished by a concentrator and an absorber placed at the focus to form a solar collector system [2]. This simple construction could be used for solar thermal technology. Moreover, simplicity and reliability are keys to the cost-effectiveness of any solar system. The four main technologies utilizing concentrated solar thermal energy are parabolic trough systems, solar tower systems, parabolic solar dish systems and linear Fresnel systems have been reviewed in [3]. Solar parabolic dish systems convert solar radiation into thermal energy, which can be used directly in solar cookers or converted to mechanical energy for water pumping or electricity generation.

*Corresponding author: AZI, S. O.
E-mail address: ogochukwuazi@uniben.edu
https://doi.org/10.60787/jnamp.vol72no.682

These systems use curved mirrors to concentrate solar radiation onto a receiver. The design of the parabolic dish considers various parameters such as reflector material, diameter, focal length, and aperture area to maximize efficiency. Solar dish systems offer advantages like high power density, efficiency, modularity, and long lifetime. These systems can operate as standalone units or be integrated into larger capacities by combining multiple units in dish farms. Solar dish systems consist of three main components: the solar dish concentrator with supporting structure, the receiver housing, and the solar tracking system. Various designs and components have been developed to optimize solar dish systems for different applications and environments. Overall, solar dish systems offer a promising and efficient renewable energy source. Researchers continue to explore and enhance these technologies to maximize their effectiveness and contribution to the renewable energy sector.

To analyze the performance of the Parabolic Dish Solar Concentrator (PDSC) system, the dish geometry needs to be studied. The factors which affect the performance of PDSC can be classified into three: design specifications, calculated and measured parameters. Also, solar radiation geometry, which depends upon the geographic and climatic conditions of the location where the PDSC system is installed, and parameters related to it affect the amount of incident solar radiation and hence, the performance of the system [4].

The optical efficiency depends on the optical properties of the dish construction materials, such as the reflectance of the dish and the optical properties of the receiver glazing, the geometry of the collector, and imperfections arising from the collector's construction. Various loss mechanisms in the collector include cosine loss, which is the ratio of the total reflective area to its projected area; shading loss, caused by the shadow cast by the receiver; reflectivity loss, representing the reflected proportion of incident energy on the reflective dish surface; transmission or absorption losses, which occur when reflected sunlight transmits through or is absorbed within the dish to the receiver; and energy spillage, which is the lost energy not captured by the receiver [5,6]. The total heat lost by the receiver includes three main types of losses: convective heat loss through the receiver aperture, radiative heat loss through the same aperture, and conductive heat loss from the receiver stand. Developing a mathematical model or thermodynamic equation to account for all these collector and receiver losses can become unwieldy. Evidently, many of the PSDC performance assessment studies have noted that a comprehensive model for losses and errors has remained a challenge [2,5,7].

A different approach, considered in this work, is to consider a PSDC as a linear system. The incident radiation and the receiver output temperature can then be transformed into the frequency domain. The system transfer function can then be obtained. From signal and systems theory, given a set of inputs the output or performance of the system can be predicted. In this work, a parabolic solar concentrator has been constructed and tested by placing a receiver filled with water at the focal point. Solar radiation and temperatures at the bottom of the receiver and water were measured and recorded. The system transfer function was calculated to predict the outcome of subsequent temperatures of the receiver and water using Fourier transformation functions in MATLAB.

2 GEOMETRY OF PARABOLA

A. The geometry of a parabola is illustrated in Figure 1.

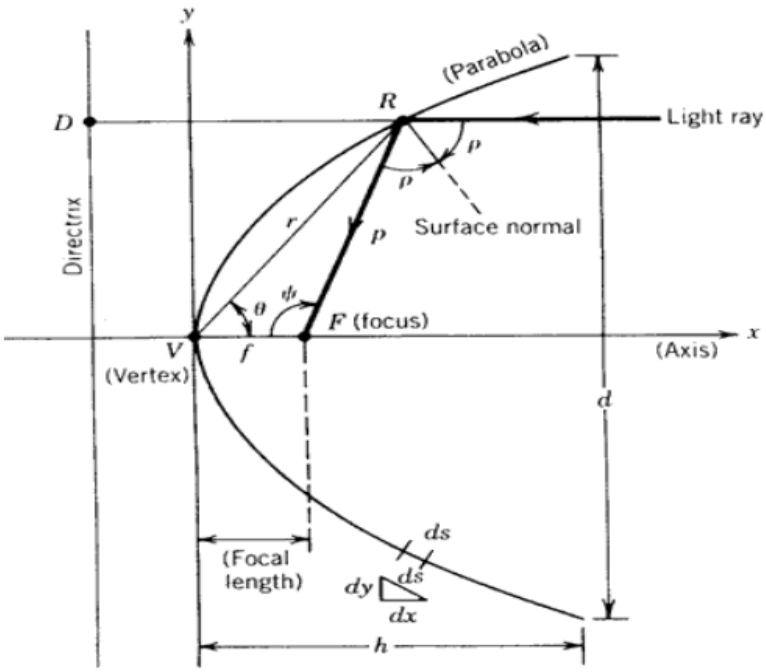

Figure 1: Geometry of a parabola (Source: [8]).

A parabola is simply the locus of points that move an equal distance from a fixed line and a fixed point. As shown in Figure 1, the fixed line is called the directrix, D, and the fixed point is the focus F. The line perpendicular to D and passing through the focus F is called the axis of the parabola. The parabola intersects its axis at a point V, which is called the vertex, which is exactly midway between the focus and D.

If the origin is taken at the vertex V and the x-axis along the axis of the parabola, the equation of the parabola is

$$y^2 = 4fx \tag{1}$$

where f, the focal length, is the distance from the vertex to the focus. When the coordinates origin is shifted to point F, as is often done in optical studies, with the vertex to the left of the origin, the equation of a parabola becomes, $y^2 = 4f(x+f)$.

In polar coordinates, using the usual definition of r as the distance from the origin and θ the angle from the x-axis to r, we have for a parabola with its vertex at the origin and symmetrical about the x-axis

$$\frac{\sin^2\theta}{\cos\theta} = \frac{4f}{r} \tag{2}$$

However, it is more useful to define the parabolic curve with the origin at F and in terms of the angle (ψ) in polar coordinates with the origin at F in solar studies. The angle ψ is measured from the line VF and the parabolic radius p, is the distance from the focus F to the curve. Shifting the origin to the focus F, we have

$$p = \frac{4fx}{1+\cos\omega} \tag{3}$$

Since solar radiation arrives at the earth in essentially parallel rays and by Snell's law the angle of reflection equals the angle of incidence, all radiation parallel to the axis of the parabola will be reflected to a single point F, which is the focus. Thus, we can write

$$\Psi = 2p \tag{4}$$

ψ is the angle of reflection and P is the distance RF from Figure 1. Solar concentrators are often a section of the infinite curve. The section is usually defined in terms of the rim angle ψ, or f/d, that is the ratio of the focal length, f, to the dish aperture diameter, d. The size of the curve is then specified in terms of a linear dimension of d or f. The rim angle, ψ, may be found in terms of the parabola dimensions as:

$$\tan\Psi_{rim} = \frac{6h}{d} \tag{5}$$

The cross sectional area of the space enclosed between a parabola and a line across its aperture and normal to the axis is given by

$$A_x = \frac{2}{3}dh \tag{6}$$

This area should not be confused with the reflecting surface area of a parabolic trough or dish or their aperture areas [9]

$$\frac{f}{d} = \frac{1}{\left\{4\tan\left(\frac{\Psi_{rim}}{2}\right)\right\}} \tag{7}$$

B. Concentration Ratio

The "concentration ratio" is used to describe the amount of light energy concentration achieved by a given collector. Two different definitions of concentration ratio are in general use. The Optical Concentration Ratio (CRo) can be calculated using Equation (8) as follows [10]

$$CR_0 = \frac{\frac{1}{A_r}\int I_r dA_r}{I_0} \tag{8}$$

where I_r represent integration over the receiver area A_r and I_o the insulation incident on the collector aperture. The Geometric Concentration Ratio can also be defined as the area of the collector aperture A_a divided by the surface area of the receiver A_r and can be calculated by Equation (9) as

$$CR_g = \frac{A_r}{A_r} \tag{9}$$

where A_a is the area of collector and A_r is the area of receiver. Optical concentration ratio relates directly to lens or reflector quality; however, in many collectors the surface area of the receiver is larger than the concentrated solar image.

3. SYSTEMS APPROACH TO THE OPERATION OF A SOLAR DISH

The Discrete Fourier Analysis theory of Linear Time Invariant Systems approach is presented here as an alternative estimation of the yield of a solar dish. This method sidesteps the detailed thermodynamic analysis and modelling with ANSYS, COMSOL and other software.

A solar dish can be viewed as a continuous system represented by

$$x(t) \quad \rightarrow \quad \boxed{\text{Continuous Time}} \quad \rightarrow \quad y(t) \tag{10}$$

or as a discrete system as

$$x[n] \quad \rightarrow \quad \boxed{\text{Discrete Time}} \quad \rightarrow \quad y[n] \tag{11}$$

where x(t) or x[n] are the inputs and y(t) or y[n] are the respective outputs.

Here it is assumed that the solar dish is a causal, linear, time-invariant (LTI) system. This model provides insight into the intricate relationship between insolation and both the receiver and water temperature. This simple representation is possible because the model can describe many other physical systems including more complex renewable energy devices. The discrete system is preferred since n represents the time stamp for available data. In general, Equation (2) can be written as

$$\sum_k a_k x_k[n] \rightarrow \sum_k b_k y_k[n] \tag{12}$$

If we regard the dish receiver module as an LTI system and the unit sample response h[n] as a system characteristic transfer function, then

$$\delta[n] \rightarrow h[n] \Rightarrow \delta[n-k] \rightarrow h[n-k] \tag{13}$$

where $\delta[n]$ describes the time factor by time –invariance.
The from LTI:

$$x[n] = \sum_{k=-\infty}^{\infty} x_k[n]\delta[n-k] \rightarrow y[n] = \underbrace{\sum_{k=-\infty}^{\infty} x_k[n]h[n-k]}_{Convolution\ \ sum} \tag{14}$$

Thus $y[n]$ can be written as a convolution of the input $x[n]$ and the system characteristic transfer function $h[n]$;

$$x[n] \quad \rightarrow \quad \boxed{\text{Discrete Time}} \quad \rightarrow \quad y[n] = x[n] * h[n] \tag{15}$$

Using Discrete Fourier Transform (DFT), $x[n] \rightarrow \mathrm{X}(e^{j\omega})$, $y[n] \rightarrow \mathrm{Y}(e^{j\omega})$ and $h[n] \rightarrow \mathrm{H}(e^{j\omega})$ where $\rightarrow$ symbolizes the respective transform operation of the input, output and system transfer function [11]. The transfer function of the dish receiver system in frequency domain can be derived from the DFT of a set of input and output data. It should then be possible to estimate the output of a system from previous inputs by convolution. This principle is well established in system analysis.

4. PARABOLIC DISH AND RECEIVER

The reflector of the experimental device consists of a solar dish of 2.35 meters opening diameter whose interior surface is covered with a reflecting layer (back-surfaced silvered glass cut into sizes of 2cm x 2cm). It reflects solar rays to the base of a receiver placed at the focal position of the concentrator. The concentrator is posed on a directional support for two axes manual tracking of the sun. The primary measure of concentrator performance is how much of the solar insolation (measure of solar radiation) arriving at the collector aperture passes through an aperture of a specified size located at the focus of the concentrator. This measure is called the concentrator or optical efficiency and is defined as,

$$\eta = E\,\rho\,\phi\cos\theta$$

where, E is the unshaded aperture area fraction which is typically more than 95% in most designs, θ the incident angle assumed to be zero, ρ the reflectance, and ϕ the capture fraction. Since the incident angle is zero, the two critical terms in the equation is the capture fraction and the reflectance. Caption fraction is the fraction of energy reflected from the concentrator to the receiver. It is the most important factor in matching a concentrator to a receiver. Capture fraction is affected by optical errors, tracking accuracy, mirror and receiver alignment and apparent size of the sun.

The receiver used has a diameter of 150mm, and is covered with a thin coat of black paint with an absorption coefficient near 0.9 located in the focal zone of the parabola. The purpose of the receiver is to absorb as much of the concentrated solar flux as possible and convert it into heat energy. The characteristics of the receiver are presented in Table 1.

Table 1: Characteristics of the receiver

Material	Flat plate steel
Receiving diameter	0.15m
Thickness	0.01m
Height	0.3m
Receiving surface	$0.0225m^2$
Geometrical concentration factor	193
Thermal conductivity λ	50.2 W/mK

The parabolic dish concentrator with a reflective surface equipped with a receiver, which was mounted on a stand 1.8m from the ground at the back of the Center for Energy Research, University of Benin. This stand served as a manual tracking system. The receiver which has an opening at one end was filled with 2 liters of water initially and then four liters as the experiment progressed. A Type-E thermocouple was attached to the bottom of the receiver at the focal point of the concentrator and connected to a digital multimeter to read temperature. The temperature of the water in the receiver was read with a mercury-in-glass thermometer. The concentrator is oriented in front of the sun according to two freedom of degrees (hour angle and declination). The sun was tracked hourly by two manual jacks under the dish. The first jack ensured the follow up of the hour angle while the second one permits movement of the concentrator according to declination angle. These angles were preset according to the number of manual turns of the nuts constructed on the jacks. This command system permits us to obtain a circular shadow of the receiver.

Figure 2: Parabolic dish with receiver at focal point of concentrator

RESULTS AND DISCUSSIONS

The relation between solar radiation and time of the day has been studied in Benin City, altitude of (80m) and longitude of (6.41). The data for solar radiation, wind speed and ambient temperature in this research work were obtained from a Davis weather station installed at the Energy Centre Building, University of Benin, Benin City, Edo State. The values of these atmospheric parameters from 24th to 28th January, 2014, labelled as Day 1 to Day 5, are plotted in Figure 3. Figure 3a shows a low insolation for Days 1 and 4 while Days 2, 3 and 5 recorded higher insolation in Figure 3b. In this geographic zone, the solar intensity is high between 10:00 AM to 15:00 PM, after this time the insolation decreases until sun set since the city lies within moderate levels of solar radiation.

Figure 4 shows the plots of solar radiation, wind speed and ambient temperature against time for the first day of the experimental work. Solar radiation averaged 320 W/m^2 and maximum ambient temperature of 29°C were recorded, resulting in the low wind speed. Furthermore, a transfer function of the insolation as input versus water temperature as output as well as receiver temperature as a second output for Day 1 was computed MATLAB and presented in Table 2. The transfer function was employed to predict the water and receiver temperatures respectively for the other days and for comparison.

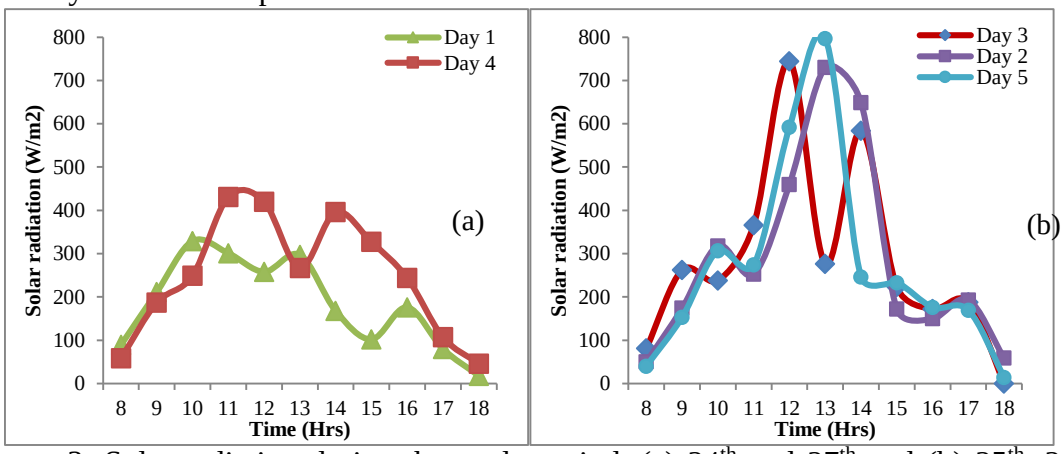

Figure. 3: Solar radiation during the study period, (a) 24th and 27th and (b) 25th, 26th and 28th January, 2014, Benin City.

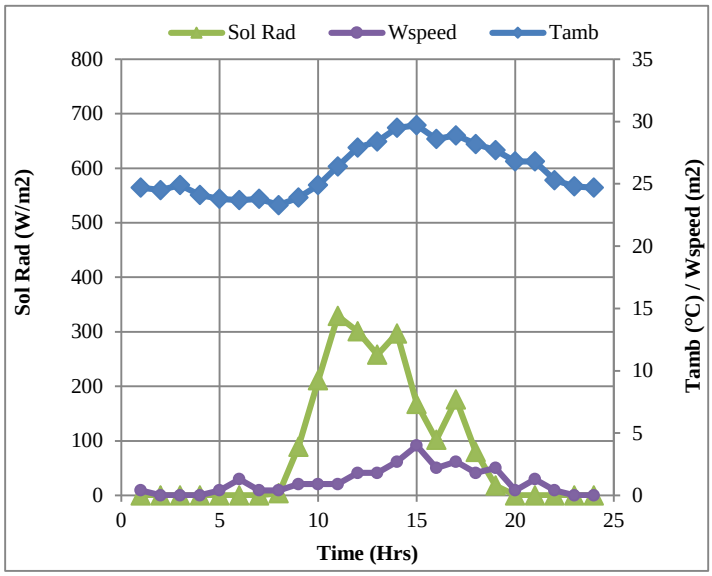

Figure 4.: Solar radiation, wind speed and ambient temperature on Day 1, 24th January, 2014.

Table 2**:** Transfer function of insolation versus water and receiver temperatures for Day 1

Day 1, 24/1/2013					
Time	Insolation (W/M^2)	Water Temp (^0C)	Water Transfer Function	Receiver Temp (^0C)	Receiver Transfer Function
10:00AM	329	31	0.1751	28.1	0.1621
10:15AM	398	32	0.0586 - 0.1255i	28.9	0.1492 - 0.1412i
10:30AM	287	36	0.0306 - 0.0245i	30.6	0.0758 + 0.0331i
10:45AM	350	40	-0.0508 - 0.0178i	34.4	-0.0490 - 0.0157i
11:00AM	301	44	0.0165 + 0.0368i	38.1	-0.0573 + 0.0594i
11:15AM	213	44	-0.0092 - 0.0145i	38.3	0.0284 + 0.0547i
11:30AM	313	44	0.0637 - 0.0583i	40.3	0.0446 + 0.1119i
11:45AM	207	45	-0.0187 - 0.0066i	40.4	0.0002 + 0.0028i
12:00PM	258	45	0.0090 - 0.0303i	58.4	-0.0145 + 0.0239i
12:15PM	542	50	-0.0090 + 0.0081i	60.6	0.0752 + 0.0786i
12:30PM	381	60	-0.0253 - 0.0066i	64.2	-0.0021 + 0.0328i
12:45PM	321	62	-0.0253 + 0.0066i	67.3	-0.0021 - 0.0328i
01:00PM	297	64	-0.0090 - 0.0081i	72.4	0.0752 - 0.0786i
01:15PM	358	63	0.0090 + 0.0303i	69.6	-0.0145 - 0.0239i
01:30PM	263	62	-0.0187 + 0.0066i	48.6	0.0002 - 0.0028i
01:45PM	306	52	0.0637 + 0.0583i	39.8	0.0446 - 0.1119i
02:00PM	168	48	-0.0092 + 0.0145i	33.1	0.0284 - 0.0547i
02:15PM	123	46	0.0165 - 0.0368i	32.7	-0.0573 - 0.0594i
02:30PM	79	42	-0.0508 + 0.0178i	30.7	-0.0490 + 0.0157i
02:45PM	63	41	0.0306 + 0.0245i	30.4	0.0758 - 0.0331i
03:00PM	102	40	0.0586 + 0.1255i	30.3	0.1492 + 0.1412i

In this work, we used the insolation as input and both receiver and water temperature as output on Day 1 to obtain the transfer function of the solar receiver system. Thus, using the transform of insolation of Day 2 as input, the put of the system in frequency domain can be obtained as [11].

$$Y_2(e^{j\omega}) = X_2(e^{i\omega})\,H(e^{i\omega})$$

Then by Inverse Fourier Transform,

$$y_2[n] \leftarrow Y_2(e^{j\omega})$$

where $\leftarrow$ symbolizes the inverse transform of $Y_2(e^{j\omega})$ to predict system output as $y_2[n]$ as shown in Figure 5. The climatic parameters are presented in Figure 5(a). Water temperature in the receiver is labeled as TW2 while the predicted water temperature as pTW2 in Figure 5(b). In a similar manner TR2 and pTR2 are for receiver temperature and predicted receiver temperatures respectively in Figure 5(c).

The dependence of receiver and water temperature on solar radiation during day time is clearly observed in the figure. Both parameters increased during day time between 10:00AM to 1:30PM because of rising solar radiation. The values peaked around 1:30 and thereafter decreased with flux of solar radiation until sunset.

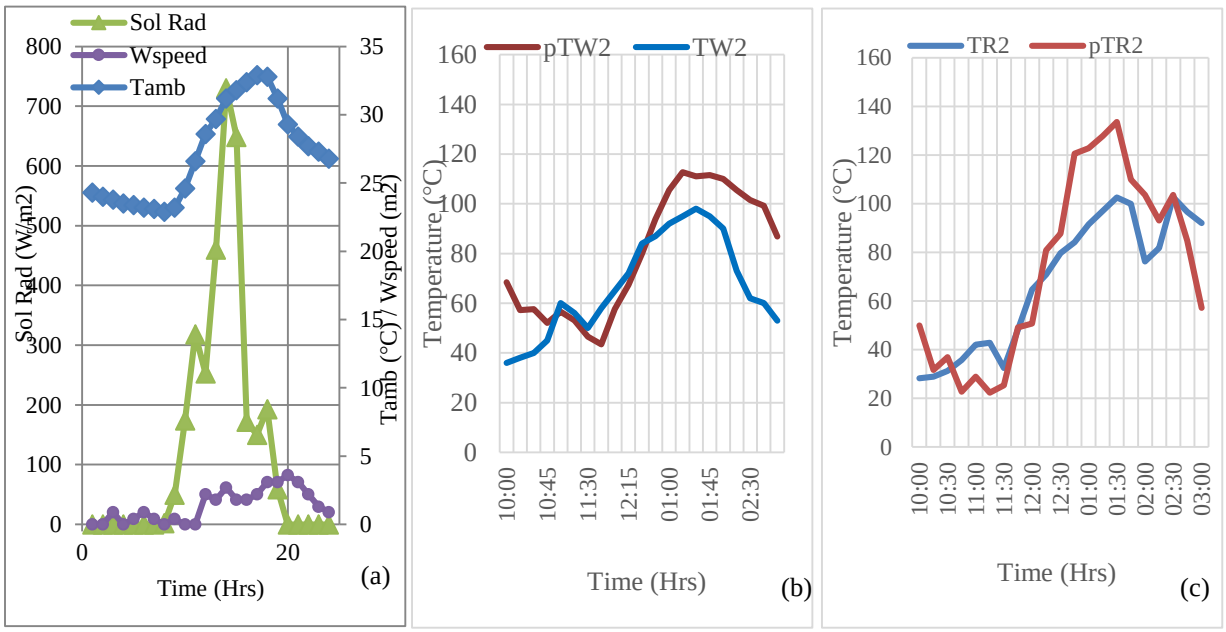

Figure 5: System Characteristics on Day 2. (a) Solar radiation, wind speed and ambient temperature, (b) water temperature and (c) receiver temperature.

The water and receiver temperatures of Days 3 to 5 were then predicted by inverse transform of the convolved insolation of the respective days and system transfer function of Day 1. The results are as presented in Figures 6 to 8. Days 2, 3 and 5 had high insolation as well as significant wind speeds. The predicted water receiver temperatures on these days showed a fairly good fit to measured values. As expected, TW2 and pTW2 gave R^2 value of 0.57 and low RMSE value or 13.56. The corresponding values for TR2 and pTR2 are 0.76 and 13.70 respectively. This can be explained from the curves in Figure 5(b) and 5(c). The curves closely follows each other between 12:00noon and 1:30PM. The residuals from observed differences did not significantly affect the statitics. TW3 and pTW3 gave R^2 value of 0.71 and low RMSE value or 10.40. Surprisingly, the corresponding values for TR3 and pTR3 are 0.21 and 23.31 respectively. This can be explained

from the curves in Figure 6(c). The curves differ by at least 20°C between 12:00noon and 1:30PM and by 30°C around 2:00PM. These differences yielded high residuals resulting in the poor statitics. Besides, on Day 3, the highest values of wind speed were recorded. Rainfall in the latter hours of the day caused low-level values in the solar radiation and ambient temperature. TW4 and pTW4 had R^2 value of 0.45 and low RMSE value or 8.57. Also, values for TR4 and pTR4 are 0.01 and 19.27 respectively. This poor correlation can be seen in Figure 7(b) and 7(c). The predicted curves are consistently higher than actual values at least 20°C all morning until 1:30PM. Again, these differences yielded high residuals. Interestingly, TW5 and pTW5 had R^2 value of 0.75 and low RMSE value or 11.67. The respective values for TR5 and pTR5 are 0.67 and 22.23 are equally notable as can be seen in Figure 8.

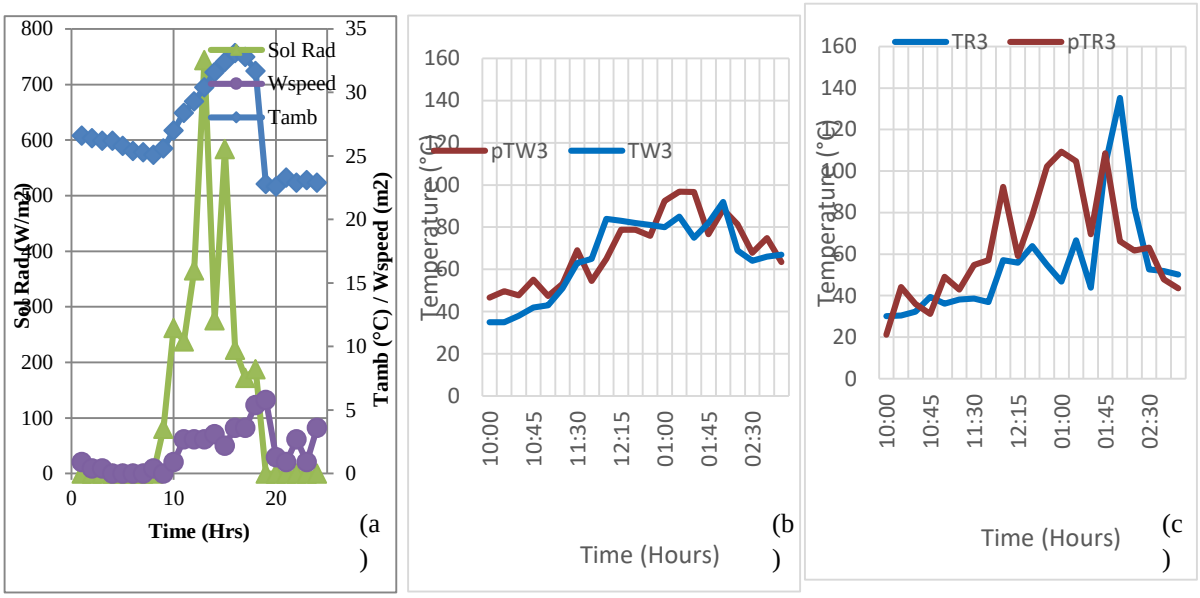

Figure 6: System Characteristics on Day 3. (a) Solar radiation, wind speed and ambient temperature, (b) water temperature and (c) receiver temperature

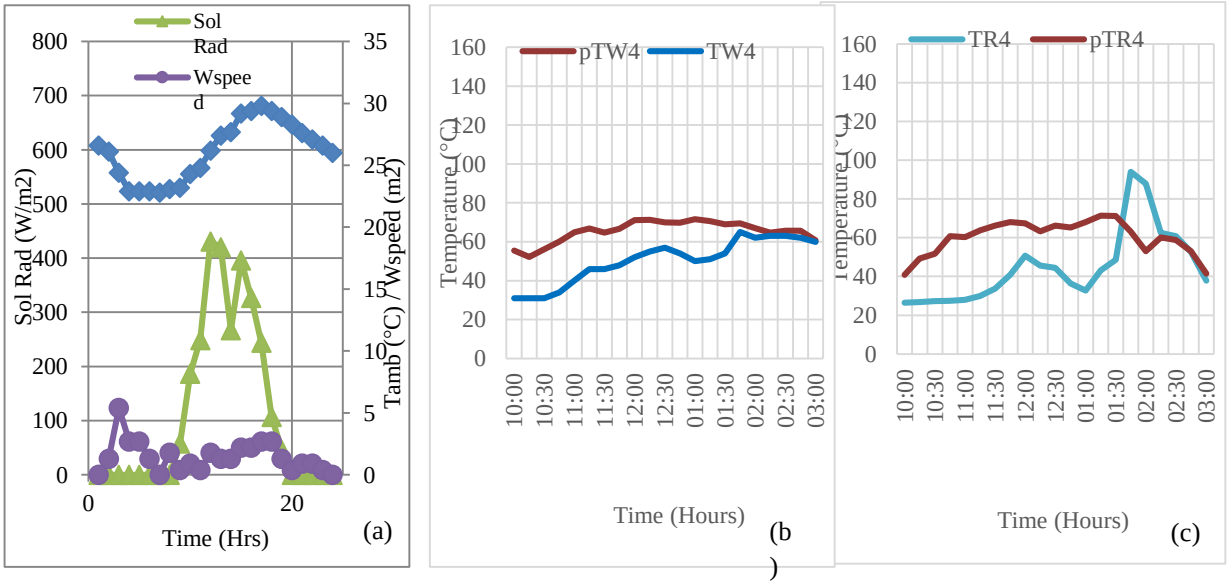

Figure 7: System Characteristics on Day 4. (a) Solar radiation, wind speed and ambient temperature, (b) water temperature and (c) receiver temperature

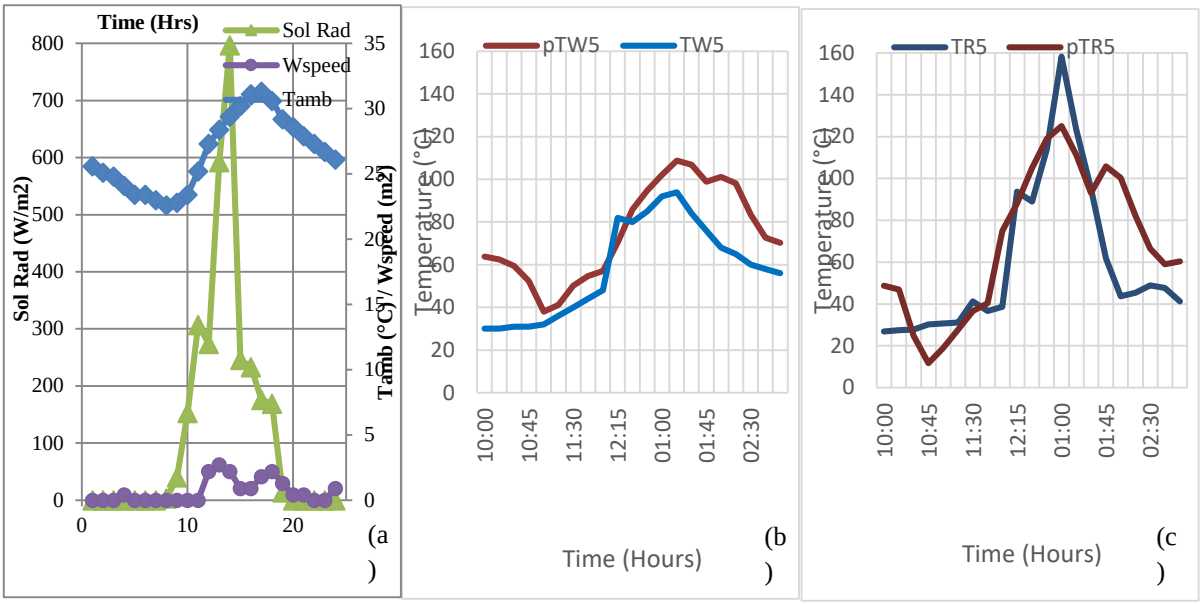

Figure 8: System Characteristics on Day 5. (a) Solar radiation, wind speed and ambient temperature, (b) water temperature and (c) receiver temperature

CONCLUSION

In this study, a parabolic solar dish concentrator has been designed. Water temperature as hot as 98 0C was achieved. This shows that the parabolic dish solar concentrator, equipped with manual tracking system and measurement of the temperature and solar power/intensity, is highly efficient in water heating applications. The temperature at the center of the receiver reached a value of about 160 °C so that fluids with lower temperature (boiling point) e.g. alcohol, can be distilled using this technology of solar energy concentration. Also, there is a good efficiency of the solar concentrator which can be increased by different interventions. In another term, using this solar equipment we can extract direct solar energy and convert it into thermal energy that can be used directly for several applications such as water heating, vapour production, etc. A fourier transformation was also carried out to obtain a transfer function for the first day i.e. Day 1 that can be used as a model to predict the succeeding water temperatures and the receiver temperatures of Day 2–5. Results showed that this predicted temperature of water and receiver followed the same trend as the original values for the water and receiver temperatures respectively.

REFERENCES

[1] Eltawi M.A., Zhengmin Z.and Yuan L. (2009). A review of renewable energy technologies integrated with desalination. Systems. Renewable and Sustainable Energy Reviews 13 (2009) pp2245-2262.

[2] Kalogirou S. A., Karellasb S., Braimakis K., Stanciuc C. and Badescud V. (2016). Exergy analysis of solar thermal collectors and processes. Progress in Energy and Combustion Science. Vol. 56, pp106-137

[3] Hafez A.Z., Soliman A., El-Metwally K.A., and Ismail I.M. (2017), Design analysis factors and specifications of solar dish technologies for different systems and applications. Renewable and Sustainable Energy Reviews. 67 pp1019–1036.

[4] Thakkar V., Doshi A., and Rana A. (2015). Performance Analysis Methodology for Parabolic Dish Solar Concentrators for Process Heating Using Thermic Fluid. IOSR Journal of Mechanical and Civil Engineering (IOSR-JMCE) Vol. 12(1) pp 101-114

[5] Kribus A, Kaftori D, Mittelman G, Hirshfeld A, Flitsanov Y, Dayan A; A miniature concentrating photovoltaic and thermal system, Energy Convers Manage, 47(20), 2006, 3582–90.

[6] Feuermann D, Gordon JM, High-concentration photovoltaic designs based on miniature parabolic dishes, Solar Energy, 70(5), 2001, 423–30

[7] Kasaeian A., Cheraghchi A, Maghdouri Z., Goodarzi K., Ranji Z. and Sara Borhani S. (2026). A comprehensive review of exergy analysis of solar parabolic dish collector systems. Energy Conversion and Management: X 29 (2026) 101462 https://doi.org/10.1016/j.ecmx.2025.101462

[8] Fareed . M. Mohamed, Auatf.S.Jassim, Yaseen. H. Mahmood, Mohamad A.K.Ahmed (2012), Design and Study of Portable Solar Dish Concentrator, International Journal of Recent Research and Review, Vol. III, September 2012 pp52-59

[9] Stine W.B. and Harrigan R. W. (1985),"Solar Energy System and design", [online].Available :.http:\\www:power from the sun.net.htm/

[10] ARPANSA-Radiation Protection Standard Occupational exposure to ultraviolet radiation, radiation protection series no.12. Australian Radiation Protection and Nuclear Safety Agency (ARPANSA), December 2006.

[11] Oppenheim A. V, Willsky A.S. and Nawab H. S. (1996). Signals and systems. 2ed. Prentice-Hall, Inc. New Jersey